MADRID
inter.noise 2019
June 16 - 19
NOISE CONTROL FOR A BETTER ENVIRONMENT

# Optimal design of the damping layer in plate with imperfect Acoustic Black Hole for wave energy dissipation

**Huang, Wei**[1]
**Ji, Hongli**[1]
**Tao, Chongcong**[1]
**Qiu, Jinhao**[1, *]
**State Key Laboratory of Mechanics and Control of Mechsanical Structures ,Nanjing University of Aeronautics & Astronautics**
**Yudao Street 29, Nanjing 210016, China**

**ABSTRACT**

**Acoustic black hole (ABH) effect in thin-walled structures provides drastic wave focalization generating local areas with high energy density. The concentrated wave energy in practical ABH structures can be dissipated by introducing a very small amount of damping layer. In this work, topology optimization of the damping layer is conducted to achieve maximum energy dissipation. The coupled model of the ABH plate with a damping layer is discretized by finite elements. The material parameters of each element of the damping layer indicating the presence or absence of material are used as topology design variables. The viscous dissipation of the damping layer under a burst tone excitation is calculated as the objective function. The optimization problem is solved using the optimality criteria. Finally, numerical results show the necessity of optimization design when the size of damping layer is small.**

**Keywords:** Acoustic Black Hole, Damping layer, Topology Optimization, Energy Dissipation
**I-INCE Classification of Subject Number:** 45

## 1. INTRODUCTION

The Acoustic Black Hole (ABH) phenomenon in thin-walled structure providing drastic wave trapping [1,2] has drawn wide attentions. Practical ABH structures always have inevitable flaws, such as truncation in one-dimensional ABH beams [3-5] or central plateau in two-dimensional ABH plates [6-8], which adversely affect the wave trapping effect. However, the imperfect ABH structures still provide local area with high energy density and strong energy focalization effect. A very small amount of damping layer introduced in the area where the energy is concentrated can effectively dissipate the

* qiu@nuaa.edu.cn

energy [3,4,9,10]. Both the energy focalization and dissipation effect of the imperfect ABH structures are of essential importance for engineering applications.

The authors' previous researches reported the energy focalization phenomenon in imperfect ABH indentations[7,8]. Specifically, the position of energy focalization is off the central part of the indentation and strongly depends on the geometrical parameters introduced by the flaws. For most of the ABH indentations, circular additional layers are conducted covering the central part of the ABH area [11,12] for wave manipulation. It can possibly lead to less effective and cost-inefficient energy utilization of the additional layers. A more reasonable layout of the damping layer, especially in the plate structures with imperfect ABH indentations, is valuable for achieving energy dissipation effect. Therefore, it is necessary to investigate the optimal design of damping layers.

The layout optimization, also called topology optimization, is conducted to design the shape and distribution of the damping layer in this work. We aim to find the damping layer that can maximize the viscous dissipation in the ABH plate. The optimality criteria (OC) method are conducted to solve the optimization problem. It is especially efficient for problems with large numbers of design variables and few constraints [13,14]. The structural topology optimization are mostly element based. The initial model of the ABH plate covered with damping layer is discretized using a finite element (FE) mesh. The viscous dissipation of each element of the damping layer is calculated using the commercial FE software ABAQUS. Section 2 is devoted to describe the topology optimization problem. In Section 3, Numerical cases and results are presented and discussed. Conclusions are drawn in Section 4.

## 2. THE TOPOLOGY OPTIMIZATION PROBLEM

To achieve maximum viscous dissipation in the imperfect ABH indentation, the damping layer is designed by topology optimization. The OC method and the FE method are combined to solve the optimization problems. The energy focalization and dissipation of ABH effect is presented in Section 2.1. The energy of viscous dissipation is the objective function which is calculated by FE method. Damping layer topology design is explained in Section 2.2.

### 2.1. Energy focalization and dissipation of ABH effect

ABH structures can be implemented by structure tailoring and material modification [15]. The gradual reduction of the flexural wave velocity results in energy focalization in ABH structures. For the bending waves in the ABH with both diminishing thickness $h(x)$ and elastic modulus $E(x)$, the local wave speed $c_b(x)$ is expressed as:

$$c_b(x) = \sqrt[4]{\frac{E(x)h^2(x)\omega^2}{12(1-v^2)\rho}} \tag{1}$$

where $\omega = 2\pi f$ is the angular frequency, $\rho$ is the density.

Damping layers are introduced to dissipate the wave energy. In FE method, the balance of energy is written as:

$$E_K + E_U = \int_0^t \dot{E}_{wf}\, d\tau + constant \tag{2}$$

where $E_K = \int_V 0.5\rho\vec{v} \cdot \vec{v} dV$ is the kinetic energy, and $E_U$ is the internal energy, $\dot{E}_{wf}$ is the rate of work done to the body. The dissipated portions of the internal energy are split off:

$$E_U = E_I + E_v = \int_0^t \left( \int_V \overrightarrow{\sigma^c} : \dot{\varepsilon}\, dV \right) d\tau + \int_0^t \left( \int_V \overrightarrow{\sigma^v} : \dot{\varepsilon}\, dV \right) d\tau \tag{3}$$

where $E_I$ is the potential energy, and the $E_v$ is the energy dissipated by viscous effects, $\overrightarrow{\sigma^c}$ is the elastic stress; $\overrightarrow{\sigma^v}$ is the viscous stress defined for material damping. Thus, the viscous dissipation of each element over time can be calculated.

### 2.2. Damping layer topology design

It is our aim to maximize the viscous dissipation of the damping layer. The objective function is written as:

$$\begin{aligned} &\min_x:\ E_v(\mathbf{x}) = \sum_{i=1}^{N} E_v(x_i) \\ &\text{S.T.}: \frac{M(\mathbf{x})}{M_0} = R_m \\ &: \mathbf{0} \le \mathbf{x}_{min} \le \mathbf{x} \le \mathbf{1} \end{aligned} \tag{4}$$

where $\mathbf{x}$ is the vector of design variables, $x_i$ is the component for the *i*th element. $N$ is the number of elements of the damping layer. $M(\mathbf{x})$ and $M_0$ are the material mass and full design domain mass when $\mathbf{x} = \mathbf{1}$, respectively. $R_m$ is a given mass ratio. $\mathbf{x}_{min} = 0.001 \cdot \mathbf{1}$ is a vector of minimum relative material parameters. The $x_i$ are relaxed so that they can take all values between $x_{min}$ and 1, which are associated with material properties of the elements including the density, Young's modulus and damping.

The optimization problem is solved using the OC method which is omitted here and can be found in the references [13,14,16]. The sensitivity of the objective function is expressed as:

$$\frac{\partial E_v}{\partial x_i} = -p x_i^{p-1} E_v(x_i)/V(x_i) \tag{5}$$

where $p = 3$ is the penalization power parameter so that the intermediate $x_i$ can be forced toward either $x_{min}$ or 1. Regions with $x_i = 1$ represent material regions, whereas regions with $x_i = x_{min}$ represent voids.

## 3. NUMERICAL CASES AND RESULTS

### 3.1. Numerical example

A plate with an imperfect ABH indentation covered with a damping layer is conducted as an example. The FE model is shown in Figure 1, the thickness of the ABH area gradually changes according to the function $h(r) = a(r - r_1)^m + h_1$. The radius $r_1$ and thickness $h_1$ of the central plateau are 0.01m and 0.3mm, respectively. The radius of the ABH is 0.1m. The size of the plate is $0.22 \times 0.22 \times 0.003$m. The design domain is the damping layer covering on the flat side of the ABH plate, the thickness of the layer is 0.001m. The mesh of the damping layer is shown in Figure 1(b), the number of the elements which is also the number of the design variables is 6128. The element type is C3D20R. A list of the material properties used in the FE model is provided in Table 1.

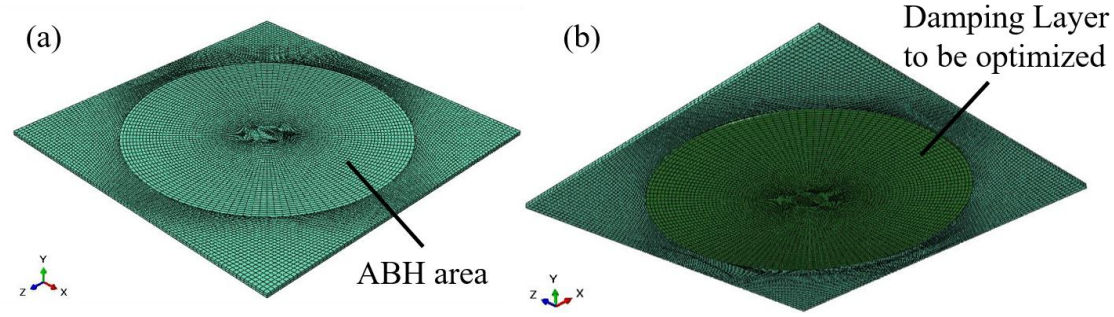


*Figure 1 FE model.*

*Table 1 Material properties.*

| | $E$(GPa) | $\rho$(kg/m$^3$) | $v$ | $\eta$ | |
|---|---|---|---|---|---|
| | | | | $\alpha$ | $\beta$ |
| Plate | 270 | 7800 | 0.3 | 0.06268 | 1.59E-9 |
| Layer | 1 | 1160 | 0.35 | 62.68 | 1.59E-6 |

The structure with power-law-profiled indentation is excited by a unit Hanning-windowed tone burst with a central frequency of 10kHz as shown in Figure 2(a). The right-hand-side edge of the plate is pinned and the excitation source is applied along the left edge as shown in Figure 2(b).

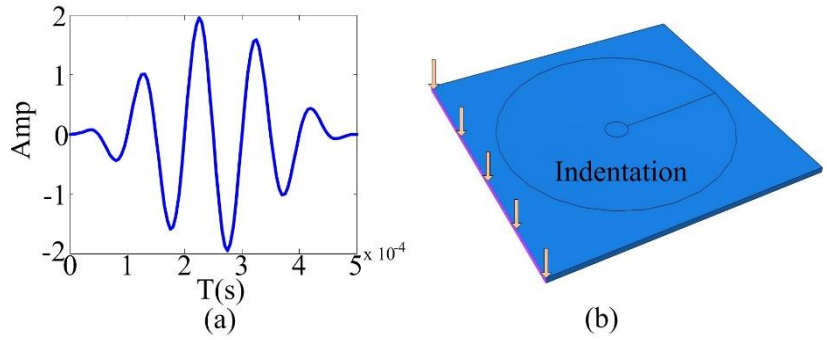


*Figure 2 Excitation signal (a) and the position of excitation (b).*

### 3.2. Results and disscusions

The numerical results are discussed in this section. An example of the initial damping layer for topological optimization is demonstrated in Figure 3. The values of design variables are mapped to the gray-scale bar. The initial damping layer is uniform and it fully covers the ABH area. Its mass ratio $R_m$ is 10%. The ABH plate with the damping layer conducted in FE method is a fully coupled model. The viscous dissipation of the whole damping layer within a time period of $0.6\text{ms}$ $(1.3\tau)$ is calculated, and $\tau$ is the time for one-way flexural wave propagation from left to the right boundary of the uniform portion. This time period is chosen because the wave energy focalization is found to remain within a period of time about $1.1\tau - 1.3\tau$ [7]. Meanwhile, the position of wave focalization is not affected by the reflection from the boundary within this time.

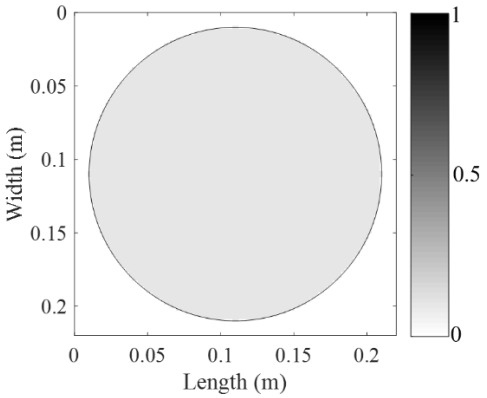


*Figure 3 Initial damping layer.*

The traditional configuration scheme of the damping layer is presented in Figure 4(a). It is a circular damping layer covering the central region of the ABH area. The distribution of the viscous dissipation of elements is shown in Figure 4(b). Figure 4(c) and Figure 4(d) demonstrate the corresponding configuration scheme of the damping layer and the results of dissipated energy after the optimization. The optimized shape of damping layer is quite clear and manufacturable since only a few elements remain 'gray' while the others become either solid or void. Moreover, the solid elements with the presence of material have excellent space continuity. By comparing the results of viscous dissipation before and after the optimization, a larger region with high dissipation efficiency is covered by the optimized damping layer. The centroid of the optimized damping layer relatively moves to downstream. It is because that the energy focalization takes place at the downstream area offset the central part in an imperfect ABH indentation [7,8]. The results show great consistency with previous researches.

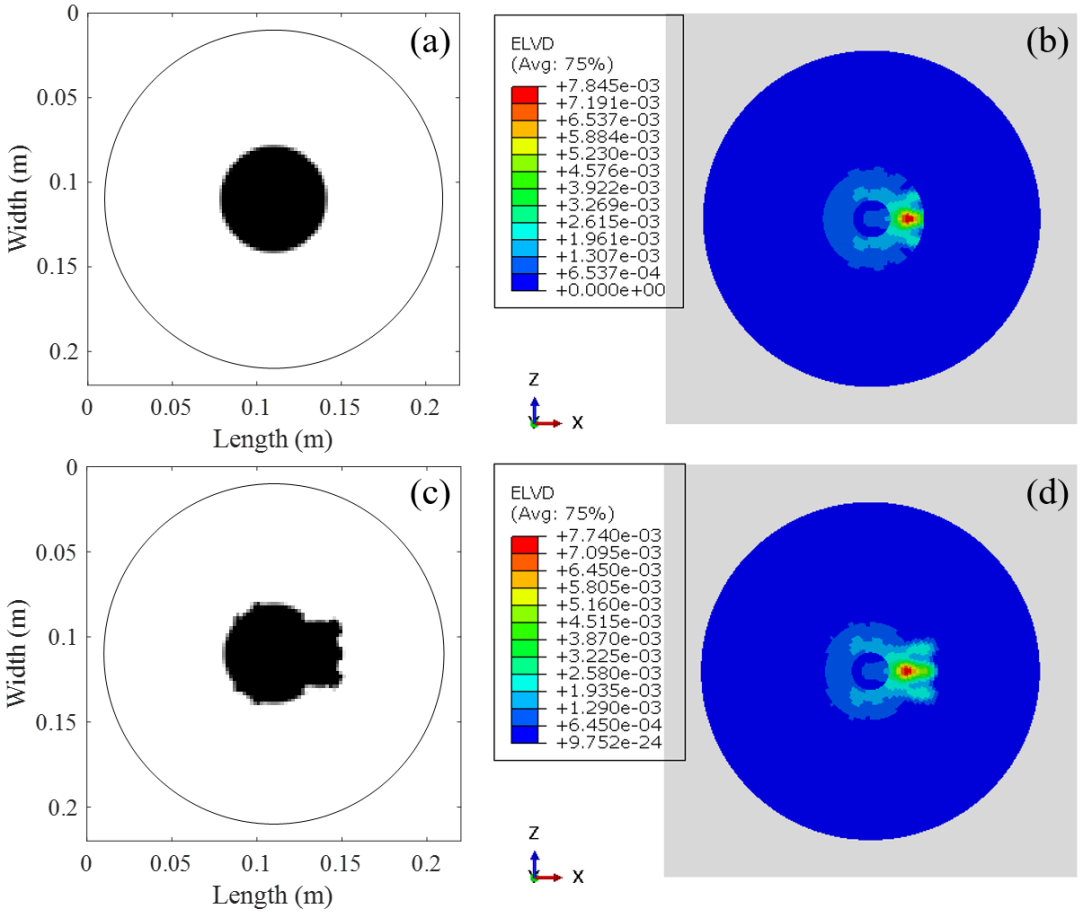


*Figure 4 Comparison of the results before and after the optimization ($R_m = 10\%$). Before: (a) configuration scheme of damping layer, (b) distribution of the viscous dissipation; After: (c) configuration scheme of damping layer, (d) distribution of the viscous dissipation.*

The comparison of the results with mass ratio $R_m$ of 1% is also presented in Figure 5. The offset of the position of the damping layer is more obvious when the mass ratio is smaller. The shape of the layer changes from a circle to a strip. From the results of the distribution of the viscous dissipation shown in Figure 5 (b) and Figure 5 (d), the energy dissipation of the elements shows significant increasing in the optimized damping layer.

To investigate the effectiveness of the optimization under different mass ratios of the damping layer from 0.05% to 50%. The normalized energy dissipation is defined as $\bar{E} = E_v/[\max(E_v')]$, $E_v'$ is the visous dissipation of the damping layer after the optimization. The improvement of the viscous dissipation is calculated as $\Gamma(R_m) = [E_v'(R_m) - E_v^0(R_m)]/E_v^0(R_m)$, $E_v^0$ is the visous dissipation of the damping layer before the optimization. Results of the visous dissipation versus mass ratio are shown in Figure 6. It can be seen from the figure that the increasing of the coverage area raises the dissipation. However, the increasing trend tends to flatten out when the mass ratio is larger than 20%. There are no evident effects on the improvement when the mass ratio is larger than 20%. However, the improvement can be above 40% when the damping layer is small, such as the mass ratio being 0.05% or 0.1%. Since the flexural waves are focused

in a very narrow area downstream of the central plateau by the ABH effect, it is easier for a larger damping layer of traditional configuration to cover the area where the wave energy is concentrated. The position of smaller optimized damping layer has more obvious deviation. Therefore, the improvement of the energy of viscous dissipation decreases with the increased mass ratio.

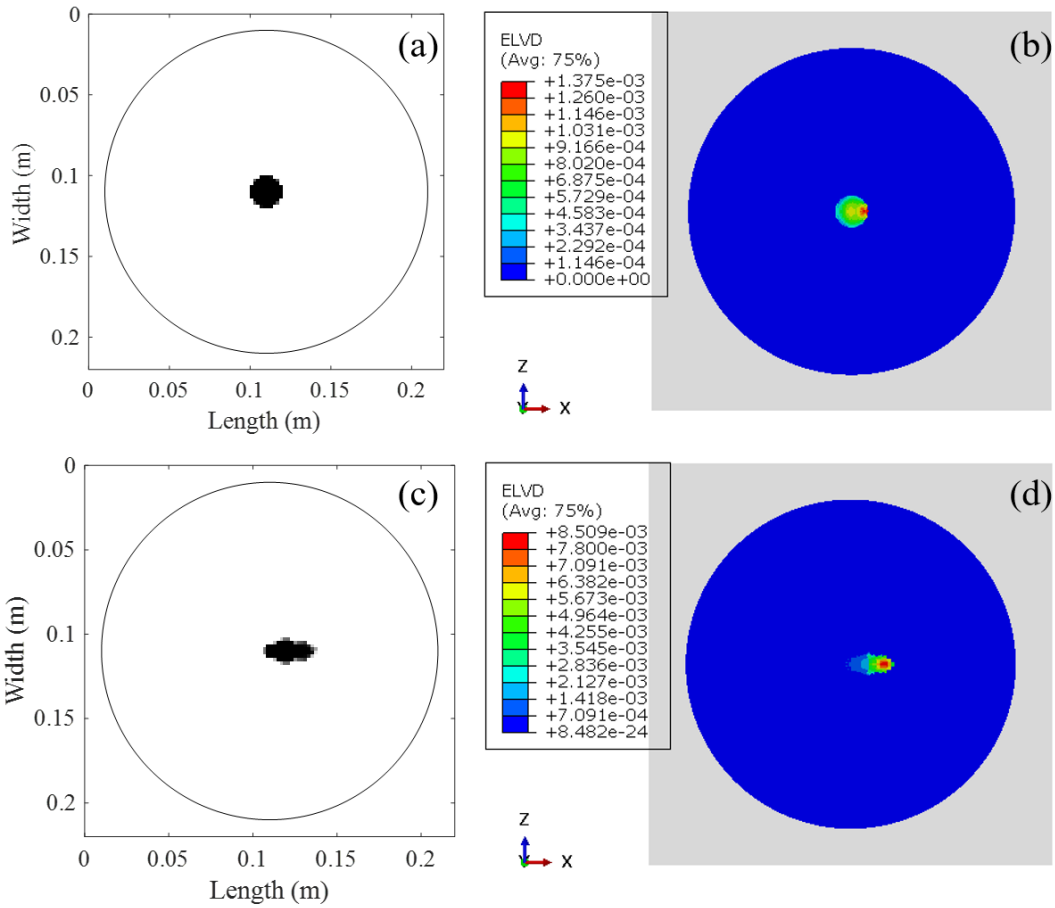


*Figure 5 Comparison of the results before and after the optimization ($R_m = 1\%$). Before: (a) configuration scheme of damping layer, (b) distribution of the viscous dissipation; After: (c) configuration scheme of damping layer, (d) distribution of the viscous dissipation.*

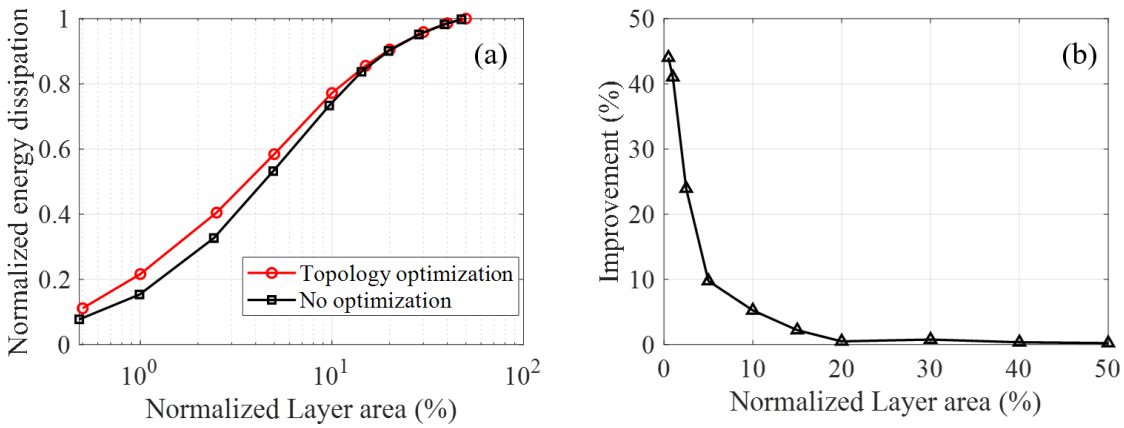


*Figure 6 Energy of viscous dissipation versus mass ratio. (a) comparison of the normalized energy dissipation before and after the optimization, (b) the improvement of the dissipation by optimization.*

## 4. CONCLUSIONS

In this paper, the damping layer in an imperfect two-dimensional ABH structure is optimally designed to maximize the energy dissipation. The topology optimization is conducted, and the optimization problem is solved by combing the FE method and the OC method. The desired layout of the damping layer in the ABH structure is achieved under a burst tone excitation. The effectiveness of the optimization with different mass ratios of the damping layer is also investigated. Comparing the energy of viscous dissipation before and after the optimization, the improvement of the viscous dissipation increases with the decrease of the mass ratio. An increase above 40% is achieved when the mass ratio of the damping layer is smaller than 0.1%.

## 5. ACKNOWLEDGEMENTS

This work is partially supported by the National Natural Science Foundation of China (Nos. 11532006 & 51775267), the Natural Science Foundation of Jiangsu Province (No. BK20181286) and the Six Talent Peaks Project in Jiangsu Province Class C (No. JXQC-002).

## 6. REFERENCES

1. M.A. Mironov, *"Propagation of a flexural wave in a plate whose thickness decreases smoothly to zero in a finite interval",* Sov. Phys. Tech. Phys. 34(3):318-319 (1988).
2. V.V. Krylov, *"Acoustic 'black holes' for flexural waves and their potential applications",* Proceedings of the Institute of Acoustics Spring Conference, Salford, UK (2002).
3. V.V. Krylov, *"New type of vibration dampers utilising the effect of acoustic black holes",* Acta Acustica united with Acustica, 90(5):830-837 (2004).
4. H. Ji, L. Jing, J. Qiu, L. Cheng, *"Investigations on flexural wave propagation and attenuation in a modified one-dimensional acoustic black hole using a laser excitation technique",* Mechanical Systems and Signal Processing, 104:19-35(2018).
5. L. Tang, L. Cheng, H. Ji, J. Qiu, *"Characterization of acoustic black hole effect using a one-dimensional fully-coupled and wavelet-decomposed semi-analytical model",* Journal of Sound and Vibration, 374:172-184 (2016).
6. E.P. Bowyer, V.V. Krylov, *"Experimental investigation of damping flexural vibrations in glass fiber composite plates containing one-and two-dimensional acoustic black holes",* Composite Structures, 107:406-415 (2014).
7. W. Huang, H. Ji, J. Qiu, L. Cheng, *"Wave Energy Focalization in a Plate With Imperfect Two-Dimensional Acoustic Black Hole Indentation",* Journal of Vibration and Acoustics, 138(6):061004 (2016).
8. W. Huang, H. Ji, J. Qiu, L. Cheng, *"Analysis of ray trajectories of flexural waves propagating over generalized acoustic black hole indentations",* Journal of Sound and Vibration, 417: 216-226 (2018).

9. V. Georgiev, J. Cuenca, M.M. Bermudez, F. Gautier, L. Simon, *"Recent progress in vibration reduction using Acoustic Black Hole effect",* In 10ème Congrès Français d'Acoustique (2010).
10. V.V. Krylov, R.E.T.B. Winward, *"Experimental investigation of the acoustic black hole effect for flexural waves in tapered plates",* Journal of Sound and Vibration, 300 (1–2):43–49 (2007).
11. L. Zhao, F. Semperlotti, *"Embedded Acoustic Black Holes for semi-passive broadband vibration attenuation in thin-walled structures",* Journal of Sound and Vibration, 388:42-52 (2017).
12. P.A. Feurtado, S.C. Conlon, *"Wavenumber transform analysis for acoustic black hole design",* Journal of the Acoustical Society of America, 140(1):718-727 (2016).
13. O. Sigmund, *"A 99 line topology optimization code written in Matlab",* Structural and Multidisciplinary Optimization, 21:120 –127 (2001).
14. B. Hassani, E. Hinton, *"A review of homogenization and topology optimization III—topology optimization using optimality criteria",* Composite Structures, 69(6):739-756 (1998).
15. W. Huang, H. Zhang, D. J. Inman, J. Qiu, C.E.S. Cesnik, H. Ji, *"Low Reflection Effect by 3D Printed Functionally Graded Acoustic Black Holes",* Journal of Sound and Vibration, 450: 96-108 (2019).
16. M.P. Bendsøe, O. Sigmund, *"Material interpolation schemes in topology optimization",* Archive of Applied Mechanics, 69(9-10):635-654 (1999).